Supernatant organics from anaerobic digestion after thermal hydrolysis cause direct and/or diffusional activity loss for nitritation and anammox

Accepted Manuscript

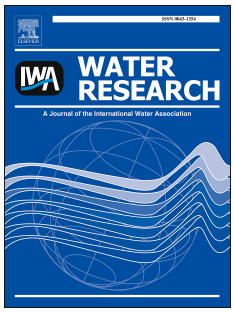

Supernatant organics from anaerobic digestion after thermal hydrolysis cause direct and/or diffusional activity loss for nitritation and anammox

Qi Zhang, Siegfried E. Vlaeminck, Christine DeBarbadillo, Chunyang Su, Ahmed Al-Omari, Bernhard Wett, Thomas Pümpel, Andrew Shaw, Kartik Chandran, Sudhir Murthy, Haydée De Clippeleir

PII: S0043-1354(18)30487-1

DOI: 10.1016/j.watres.2018.06.037

Reference: WR 13864

To appear in: *Water Research*

Received Date: 14 March 2018

Revised Date: 5 June 2018

Accepted Date: 16 June 2018

Please cite this article as: Zhang, Q., Vlaeminck, S.E., DeBarbadillo, C., Su, C., Al-Omari, A., Wett, B., Pümpel, T., Shaw, A., Chandran, K., Murthy, S., De Clippeleir, Haydé., Supernatant organics from anaerobic digestion after thermal hydrolysis cause direct and/or diffusional activity loss for nitritation and anammox, *Water Research* (2018), doi: 10.1016/j.watres.2018.06.037.

Supernatant organics from anaerobic digestion after thermal hydrolysis cause direct and/or diffusional activity loss for nitritation and anammox

Qi Zhang[1,2,3], Siegfried E. Vlaeminck[2,4,*], Christine DeBarbadillo[1], Chunyang Su[1], Ahmed Al-Omari[1], Bernhard Wett[5], Thomas Pümpel[6], Andrew Shaw[7], Kartik Chandran[3], Sudhir Murthy[1] and Haydée De Clippeleir[1]

1. DC Water, 5000 Overlook Ave. SW, Washington, DC 20032, USA

2. Center for Microbial Ecology and Technology (CMET), Faculty of Bioscience Engineering, Ghent University, Coupure Links 653, 9000 Gent, Belgium

3. Department of Earth and Environmental Engineering, Columbia University, 500 West 120th Street, New York, USA

4. Research Group of Sustainable Energy, Air and Water Technology, Department of Bioscience Engineering, University of Antwerp, Groenenborgerlaan 171, 2020 Antwerpen, Belgium

5. ARAconsult, Unterbergerstr.1, A-6020 Innsbruck, Austria

6. Institut für Mikrobiologie, Technikerstr. 25, A-6020 Innsbruck, Austria

7. Black & Veatch, 8400 Ward Parkway, Kansas City, MO 64114, USA

* Corresponding author: siegfried.vlaeminck@uantwerpen.be

Abstract

Treatment of sewage sludge with a thermal hydrolysis process (THP) followed by anaerobic digestion (AD) enables to boost biogas production and minimize residual sludge volumes. However, the reject water can cause inhibition to aerobic and anoxic ammonium-oxidizing bacteria (AerAOB & AnAOB), the two key microbial groups involved in the deammonification process. Firstly, a detailed investigation elucidated the impact of different organic fractions present in THP-AD return liquor on AerAOB and AnAOB activity. For AnAOB, soluble compounds linked to THP conditions and AD performance caused the main inhibition. Direct inhibition by dissolved organics was also observed for AerAOB, but could be overcome by treating the filtrate with extended aerobic or anaerobic incubation or with activated carbon. AerAOB additionally suffered from particulate and colloidal organics limiting the diffusion of substrates. This was resolved by improving the dewatering process through an optimized flocculant polymer dose and/or addition of coagulant polymer to better capture the large colloidal fraction, especially in case of unstable AD performance. Secondly, a new inhibition model for AerAOB included diffusion-limiting compounds based on the porter-equation, and achieved the best fit with the experimental data, highlighting that AerAOB were highly sensitive to large colloids. Overall, this paper for the first time provides separate identification of organic fractions within THP-AD filtrate causing differential types of inhibition. Moreover, it highlights the combined effect of the performance of THP, AD and dewatering on the downstream autotrophic nitrogen removal kinetics.

Keywords: biological nutrient removal, partial nitrification/anammox, water resources recovery facility

1 Introduction

Thermal hydrolysis processes (THP) are well-established as reliable and energy-efficient ways to intensify solids handling in sewage treatment, by creating a change in the rheology of the waste sludge which allows for increased loading rates resulting in smaller digester volumes (Barber 2016). In addition, this technology lowers the bound water fraction in sludge, thus resulting in an increased cake solids concentration after dewatering irrespective of dewatering equipment (Bader 1978, Jolis 2008, Pickworth et al. 2006). The combination of THP and anaerobic digestion (AD) has been applied worldwide, e.g. at HIAS wastewater treatment plant (WWTP) (Hamar, Norway), Hengelo WWTP (Hengelo, The Netherlands), Oxley Creek Water Reclamation Plant (Australia) and Blue Plains Advanced WWTP (DC Water, Washington, DC, USA) (Dwyer et al. 2008, Pickworth et al. 2006). The rapid decompression due to releasing steam reduces the sludge particle size by 40-50%, while higher levels of colloidal and particulate organics were observed in the returned liquor compared to the returned liquor from conventional AD (Barber 2016, Bougrier et al. 2008, Feng et al. 2014, Haug 1978, Zhang et al. 2016). This can potentially be resolved by adding coagulants which enhance the capture of fine solids or by allowing for enhanced flocculation under optimized combinations of shear and exposure time (Niu et al. 2013, Poon and Chu 1999).

Deammonification or partial nitritation/anammox is well established as resource-efficient nitrogen removal process with 100+ full-scale applications, and is particularly suitable to treat dewatering liquor from sludge AD (Lackner et al. 2014). Most observed limitations in performance have been associated with aerobic ammonium-oxidizing bacteria (AerAOB) due to sensitivity towards organics substances, micronutrient limitation or free ammonia inhibition (Gujer 2010, Sinha and Annachhatre 2006). Limitations on anoxic ammonium-oxidizing or anammox bacteria (AnAOB) because of similar factors are mostly compensated by efficient (and enhanced) retention of AnAOB, creating a larger buffer in AnAOB biomass (Han et al. 2016). In recent years the application of deammonification has stepwise been expanded to treat livestock wastewater (diluted), landfill leachate, and THP digestate. All these

types of wastewater contain a wider range of inorganic and organic compounds compared to conventional sewage sludge AD effluent, with reported challenges for efficient and stable deammonifaction treatment (Dapena-Mora et al. 2006, Ganigué et al. 2008, Kindaichi et al. 2016, Lotti et al. 2012, Zhang et al. 2016). For THP, cell lysis under the high temperatures yields AD filtrate higher in organic compounds concentration (Barber 2016), which has shown to be (partially) inhibitory towards AerAOB and AnAOB (Figdore et al. 2011), challenging efficient N removal (Chan, 2015; Zhang et al., 2016). When comparing deammonification treatment of conventional AD filtrate with treatment of THP-AD filtrate in two long-term reactors, decreased AerAOB rates were observed when treating THP-AD filtrate, potentially caused by increased level of organics present in THP-AD filtrate (Zhang et al., 2016). Optimization of key control parameters enabled efficient treatment, including increased dissolved oxygen (DO) set-point (1 mg O_2/L), longer aeration times and selective AnAOB retention through screens (Zhang et al. 2016). When AD instability yielded increased digestate concentrations of volatile fatty acids and other organics, these soluble and colloidal compounds decreased the deammonification performance considerably (Zhang et al., 2016). The link between THP and creation of inhibitory compounds was also observed at full-scale, with the performance of sidestream deammonification decreasing after upstream implementation of THP (Chan 2015). However, to the best of our knowledge, no specific inhibitory factors have yet been identified within THP-AD filtrate, nor have the inhibition mechanisms for AerAOB and AnAOB been unraveled.

Monod microbial growth kinetics are the simplest and most popular rate expression, assuming that every single essential substrate is a growth-limiting factor (Beg and Hassan 1987, Han and Levenspiel 1988). To include inhibition-related limitations in growth rate, Monod-type models were further developed based on three ways of inhibition (Han and Levenspiel 1988): (i) competitive inhibition, yielding an increased substrate affinity constant (K_S) but not affecting the maximum specific growth rate (μ_{max}), (ii) non-competitive inhibition, lowering μ_{max} but not impacting K_S, and (iii) uncompetitive inhibition, combining aspects of non-competitive and competitive inhibition, i.e. affecting both K_S and

89 μ_{max}. Interestingly, recent work of Shaw et al. (2015) has shown that K_S is not a constant, but the
90 maximum rate and diffusion influence this parameter with a relationship established based on a linear
91 data fit and the porter-diffusion model. This concept was shown to be widely applicable, as shown by
92 fits for denitrification (biofilm and floc), nitrification and anaerobic digestion (Shaw et al. 2015).
93 Summarizing, inhibitors can be described as (i) direct, causing decreased microbial growth rates hereby
94 assuming inhibitors do not influence the diffusion to the cells (i.e. non-competitive inhibition), by using
95 an 'inverted' Monod factor of the so-called direct inhibitor, and (ii) diffusional (indirect), limiting
96 diffusion represented by an increased K_S value (i.e. competitive inhibition), through including the
97 porter-equation on the affinities for substrate and direct inhibitors. In the case of THP-AD filtrate,
98 diffusion limitation on AerAOB containing flocs caused by the increased particulate and colloidal
99 fractions was suggested to be responsible for decreased ammonium conversion rates (Zhang et al.,
100 2016). Inclusion of this mechanism in a model is hypothesized to improve the predictability of
101 deammonification performance.

102 The first objective of this study was to identify the short-term inhibition effects and mechanisms
103 exerted by the soluble, colloidal and particulate organics in THP-AD filtrate on AerAOB and AnAOB
104 activities. Hereto, batch experiments were performed using non-acclimated deammonification sludge.
105 Tests related to examining whether inhibition was linked to: 1) quality of the THP-AD filtrate, 2)
106 additional pretreatment options, 3) performance of the dewatering stage (flocculant/coagulant polymer
107 dose). The second objective was to develop and evaluate a microbial kinetic model, identifying specific
108 contributions of organic fractions to either direct or diffusional limitations in conversion activities, both
109 for AerAOB and AnAOB.

110

111 **2 Materials and methods**

112 **2.1 THP-AD reactors**

113 Anaerobic sludge for dewatering was obtained from two types of AD systems. Firstly, a semi-technical
114 scale (60 L) reactor was used, fed with thermally hydrolyzed sludge (at 165°C, 30 min) (DC Water,
115 Washington, DC, USA). This digester was stably operated at 15 days solids retention time (SRT), with
116 a feed total solids (TS) concentration of about 10.5% yielding 50% volatile solids (VS) reduction at
117 38.5±1°C. Secondly, one of the four full-scale anaerobic digesters was sampled, which was started up
118 in October 2014 with an increasing feed loading from the same THP process. The digesters were
119 operated around 20 days SRT at 38°C, fed with 9.5% TS with 70% VS reduction.

120

121 **2.2 Sludge dewatering: filtrate production**

122 The AD sludge was dewatered including rapid mixing, flocculation and belt press shear, followed by
123 gravity drainage through a belt filter cloth. The remaining solids were mechanically dewatered using a
124 centrifuge at 3000 g for 10 min (Higgins et al., 2014). FLOPAM 4440 (SNF, GA, USA), a
125 polyelectrolyte with a very high molecular weight and median cationic charge (35%) was used as
126 flocculation polymer. The optimal polymer dose (OPD) was determined based on filtrate quality by
127 establishing a polymer dosing response curve, which varies depending on the digester operation
128 conditions.

129

130 **2.3 Description of filtrate applied in the tests**

131 **2.3.1 Filtrate quality at digester stability and unstability**

132 The lab-scale digester was stably operated for two years, to compare to the full-scale digesters (Zhang

et al., 2016). For the full-scale digesters, representative samples were obtained for unstable and stable behavior. The unstable full-scale AD refers to inconsistent loading and inadequate mixing in the digester one month after reaching its full loading rate. During this event, the digesters experienced foaming, increased volatile fatty acids (VFA) concentrations, and decreased pH, alkalinity, specific gravity and biogas methane content. Four months after the digesters recovered from the unstable period mentioned above, another sludge sample was taken and underwent the same inhibition activity tests, referred to in this study as stable full-scale AD.

2.3.3 Filtrate pretreatment procedures

Five procedures were tested to remove specific classes of inhibiting components prior to the activity tests. First, micronutrient addition in the filtrate was tested to check the growth limitation. Secondly, the effect of biodegradable compounds was examined. A one-day aerobic treatment was executed, aerating the full-scale filtrate for one day in the presence of nitrifying activated sludge (3-4 g TSS/L), aiming to remove VFA and some other readily biodegradable organics. Then, long-term aerobic and anaerobic treatment were performed to remove biodegradable COD (bCOD). In the aerobic pretreatment the full-scale filtrate was aerated at a dissolved oxygen (DO) level above 4.0 mg O_2/L for seven days after addition of nitrifying activated sludge (3-4 g TSS/L), until no decrease in soluble COD was observed for the last four days. In the anaerobic pretreatment, sludge was derived from biochemical methane potential tests until only refractory COD remained in the sludge after twelve days inoculation (Stuckey and McCarty, 1984). Thirdly, precipitation with Fe^{3+} and Zn^{2+} was tested. Iron(III) sulfate (1 g Fe/L) or zinc sulfate (1 g Zn/L) was added under pH control, after which precipitates were removed by centrifugation (10 000 g, 10 min). Fourthly, filtrate was added to hexane as extraction solvent on 1:2 volume basis, followed by shaking and re-separation in a separatory funnel. Finally, adsorption to activated carbon was investigated, by adding biochar (PA, USA) and granular activated carbon (Donau

Chemie, Austria) to the filtrate, stirring the mixture for 30 min, and removing with centrifugation (10 000 g, 10 min).

2.3.4 Addition of $FeCl_3$ and polyDADMAC as coagulants

Two conditioning processes were used to alter the COD fractions in the filtrate composition, i.e. flocculation and coagulation-flocculation. As coagulants, $FeCl_3$ and polyDADMAC were injected before the addition of flocculant polymer at the rapid mixing stage. polyDADMAC (SNF FLOQUAT 4520), a very highly charged cationic polymer with a high molecular weight in a liquid form, was added as additional coagulant polymer (SNF, GA, USA**)**.

2.4 Microbial inhibition assays

The sludge used in activity test originated from a semi-technical sidestream deammonification sequencing batch reactor (SBR) located in Blue Plains (Zhang et al. 2016). Batch experiments were performed to determine the inhibition factors of THP-AD filtrate on the AnAOB and AerAOB activities. To avoid any impact of high ammonium or free ammonia levels, 2/3 of the ammonium in the reject water was stripped out at an increased pH of 10 (NaOH addition), after which the pH was corrected to 7.5 (H_2SO_4 addition). Chemical oxygen demand (COD) fractionations were measured showing that the difference before and after stripping was less than 10%, i.e. in the range of measurement error. All experiments started with 280 mg NH_4^+-N/L, 2500 mg $CaCO_3$/L as alkalinity and 20 mg NO_2^--N/L (in anoxic tests). An extra inhibition test was done to see the combined impact of ammonium and COD, thus without ammonia stripping. A synthetic medium of the same osmotic strength and ammonium content (1500 mg NH_4^+-N/L) as the THP-AD filtrate was prepared, replacing a

179 certain percentage of THP-AD filtrate on a volume basis. The AerAOB and AnAOB inhibition were
180 derived from comparing conversion rates in the treatments with filtrate to the control sets (no filtrate).

181

182 **2.5 COD fractionation, other chemical analyses and calculation methods**

183 Four fractions were considered within total COD (COD_{tot}), based on four COD measurements per
184 sample: COD_{tot} and dissolved COD (COD_{diss}) were directly measured, and particulate COD (COD_{part}),
185 large colloidal COD (COD_{coll-L}), and small colloidal COD (COD_{coll-S}) were indirectly derived based on
186 two additional measurements. COD_{part} (>1.0 µm) was obtained by subtracting the concentration after
187 direct 1.0-µm filtration (Whatman, GE healthcare, UK) of the raw sample. COD_{diss} was considered as
188 the fraction that was not retained after flocculation ($ZnSO_4$) and filtration of colloids over 0.45-µm, so-
189 called flocculated/filtered COD. COD_{coll-S} (flocculated/filtered - 0.45-µm) was obtained by subtracting
190 COD_{diss} from the value obtained after direct 0.45-µm filtration of the raw sample. COD_{coll-L} (0.45-1.0-
191 µm) was derived using filtration over 1.0-µm and subsequent subtraction of COD_{diss} + COD_{coll-S}.

192 Sludge TS, cake solids TS, total suspended solids (TSS) and volatile suspended solids (VSS) were
193 measured according to standard methods (American Public Health Association, 1999). NH_4^+, NO_2^-,
194 NO_3^- and COD were measured spectrophotometrically using Hach vial kits (DR-2000, Hach, CO,
195 USA). Volatile fatty acids (VFA) were measured using gas chromatographic (GC) methods (Lu et al.,
196 2015).

197

198 **2.6 Model description and comparison**

199 Two classes of models were used using the results from 97 batch experiments to estimate inhibitor
200 affinities on AerAOB and AnAOB. Model class 1 was based on direct biological inhibition, altering the

values of the maximum growth rate (μ_{max}) and inhibitor affinity (K'_I) to quantify the effects of direct inhibitors (I), assuming that diffusion limitations are constant, i.e. independent of the inhibitor(s) (Han and Levenspiel, 1988). Model 1a used the conventional approach**.**

$$\mu = \mu_{max} * \left(\frac{S}{S + K'_S}\right) * \left(\frac{K'_I}{I + K'_I}\right) (eq.\ 1)$$

In which:

- μ_{max}: Maximum specific growth rate (1/day),
- S: Substrate concentration (mg/L),
- I: Concentration of direct inhibitors, influencing growth rate but not changing diffusion resistance (mg/L),
- K'_S: Apparent affinity coefficient for S (mg/L),
- K'_I: Apparent affinity coefficient for I (mg/L).

Model 1b additionally used a minimum function (MIN) to take the individual impact of each fraction into account, describing the rate-limiting step as the determining factor, following the approach by Stewart et al. (2017).

$$\mu = \mu_{max} * \mathrm{MIN}\left[\left(\frac{S}{S + K'_S}\right); \left(\frac{K'_I}{I + K'_I}\right)\right] (eq.\ 2)$$

Model class 2 additionally included a mechanistic underpinning of diffusional limitations caused by diffusional inhibitors (I_d). To predict the differential inhibition effect by direct and diffusional inhibitor types, respectively I and I_d, a porter-diffusion formula was included adjusting apparent affinities for

218 substrate (K'_S) (eq.3) and direct inhibitors (K'_I) (eq.4) with diffusivities (D'_S and D'_I) determined by
219 inhibition switching functions (eq.1) (Shaw et al. 2015) (see supplementary material S1).

$$K'_S = K_{S0} + R_{max} * \frac{r_0^2}{3 * \emptyset * Sh * D'_S}; \text{with } D'_S = D_S * \frac{K_{I_{d1}}}{K_{I_{d1}} + I_{d_1}} * \frac{K_{I_{d2}}}{K_{I_{d2}} + I_{d_2}} * \dots \text{(eq. 3)}$$

$$K'_I = K_{I0} + R_{max} * \frac{r_0^2}{3 * \emptyset * Sh * D'_I}; \text{with } D'_I = D_I * \frac{K_{I_{d1}}}{K_{I_{d1}} + I_{d_1}} * \frac{K_{I_{d2}}}{K_{I_{d2}} + I_{d_2}} * \dots \text{(eq. 4)}$$

220 In which:

221 • I_{d_i}: Concentration of diffusional inhibitor I, changing diffusion resistance but not affecting
222 growth rate (mg/L),
223 • K_{S0}: Intrinsic affinity coefficient for S; near zero in comparison to diffusion resistance, thus
224 usually neglected (mg/L),
225 • K_{I0}: Intrinsic affinity coefficient for I; near zero in comparison to diffusion resistance, thus
226 usually neglected (mg/L),
227 • K'_S: Apparent affinity coefficient for S (mg/L), already including porter equation,
228 • K'_I: Apparent affinity coefficient for I (mg/L), already including porter equation,
229 • $K_{I_{di}}$: Diffusion inhibition affinity coefficient caused by I_{d_i} (mg/L),
230 • D_S: Diffusivity of S within the given biomass characteristics (m^2/s),
231 • D'_S: Modified diffusivity of S due to I_{d_i} (m^2/s),
232 • D_I Diffusivity of I within the given biomass characteristics (m^2/s),
233 • D'_I: Modified diffusivity of I due to I_{d_i} (m^2/s),
234 • R_{max}: Maximum volumetric growth rate (mg/L/d),
235 • r_0: single cell radius (m),
236 • Sh: Sherwood number, to account for convective mass transport compared to diffusive mass

transport (-), assumed to be 1.0 in all cases,

- ∅: Shape factor, to non-spherical cell (-), assumed to be 1.0.

The actual diffusivities (D'_S and D'_I) are immediately impacted by I_d during short-term exposure, and this work focused on the change of K'_S and K'_I due to particulates and large colloids. All other parameters such as r_0, Sh and ∅ were considered constant as activity tests were performed in a short-term and were cancelled out in the model fitting (See supplementary material S1). The values for S, I and K_S (not impacted by diffusion) were set using values in the batch tests, while μ_{max} and K_I were fitted. For AerAOB, the oxygen affinity coefficient K_{O2} was set at 0.25 mg O_2/L (Al-Omari et al. 2015), and S_{O2} = 3.5 mg O_2/L during the test. For AnAOB, the nitrite affinity coefficient K_{NO2-} was set at 0.5 mg NO_2^--N/L (Al-Omari et al. 2015), and S_{NO2-} = 20 mg NO_2^--N/L during the test. All other non-limiting substrates, e.g. $NaHCO_3$ and NH_4^+, were not taken into account in the tests.

As all COD fractions were interlinked, principal component analysis (PCA) was firstly used for statistical analysis to describe and summarize the dataset by reducing the dimensionality and providing deeper understanding the correlation between variables using 'FactoMineR' package in R software (Francois Husson et al. 2018). Secondly, 'minpack.lm' and 'nlstools' packages in R software were used to find the best fit and standard error of values of each model (Florent Baty et al. 2015, Timur V. Elzhov et al. 2016). Lastly, the goodness of the model fitting was quantified in three ways, by comparing the total squared error (TSE), the mean squared error (MSE) and a statistical F-test. The last indicates whether the fit of different models was significantly different, shown by a probability number (p-value) smaller than or equal to 0.05.

3 Results

The fractionation of organics in THP-AD filtrate was as follows (belt filter press operation from January to June 2015): 12±8% particulate (620±402 mg COD_{part}/L), 15±5% colloidal, of which 5±3% large colloids and 12±6% small colloids (211±155 mg $COD_{colloidal\text{-}l}$/L and 458±198 mg $COD_{colloidal\text{-}S}$/L), and 73±8% soluble organics (3575±930 mg COD_{diss}/L). To elucidate the inhibitory impacts of different COD fractions within the THP-AD filtrate, samples were taken from different AD systems (lab & full-scale), operational periods (stable & unstable), with different pretreatment methods and different dewatering conditions.

3.1 Impact of anaerobic digester performance: VFA and other biodegradable organics

Three different types of filtrate from the lab-scale (stable) and full-scale (stable and unstable) ADs were used in the tests to evaluate the impact of digester performance. The filtrate composition of the samples is shown in Table 1. Although COD_{diss} was similar between the lab- and full-scale system during stable operation, the full-scale AD had slightly higher particulate and colloidal COD concentrations. The comparison showed no significant difference in AerAOB inhibition under stable anaerobic digestion (Fig. 1a). An additional test was performed at the original ammonium concentration from the stable full-scale AD filtrate (1500 mg N/L instead of constant 280 mg N/L), allowing higher volume exposures to be tested. This showed a similar inhibition degree as the one with lower ammonium levels (Fig. 1a). Overall, AerAOB lost 50% of its activity when exposed to 40% of lab-scale AD filtrate, 46% of full-scale AD filtrate (lower ammonium/free ammonia concentration) and 30% of full-scale AD filtrate (higher ammonium/free ammonia concentration) respectively (Fig. 1a). In contrast for AnAOB, significantly higher inhibition was observed when exposed to filtrate from full-scale AD resulting in no measurable

AnAOB activity at 25% volume exposure of filtrate, while in case of the lab-scale digester still 54±5% AnAOB activity remained (Fig. 1b).

When the digester showed instability as characterized by VFA accumulation and decreased biogas production, all COD concentrations increased (Table 1 I). The largest increase was in COD_{diss}, of which 25% was due to the increase of acetate as the main VFA present (from < 100 mg COD/L to 1383 mg COD/L). The increase of COD due to the digester instability resulted in statistically higher inhibition on AerAOB and AnAOB (Fig. 1a;b). Residual AnAOB activity was less than 10% when exposed to 10% of the unstable filtrate (Fig. 1b), indicating that AnAOB were highly sensitive to the digester performance. AerAOB activity decreased initially only slightly by 11±5% at 10% of filtrate volume exposure. However, activity loss was more substantial at higher exposure (30±4% of residue activity at 46% volume exposure) (Fig. 1c). Since a considerable acetate level was observed in the unstable AD filtrate, an extra test was performed spiking acetate to stable AD filtrate (10%), reaching a similar final concentration of 1250 mg acetate-COD/L. This yielded statistically the same result (Fig. 1c;d), indicating the acetate did not contribute to the additional inhibition observed in unstable AD filtrate.

3.2 Impact of pretreatment

The first pretreatment tests examined the biodegradability of the inhibitory organics. The filtrate was treated aerobically for 1-day to verify the impact of short-term aeration, removing mainly VFA and some readily biodegradable organics (COD_{diss} decreased from 3574 to 1948 mg COD/L). The results showed that inhibitions on AerAOB and AnAOB were not significantly reduced compared to non-treated full-scale AD filtrate (stable) (Fig. 1c;d). To investigate the impact of all biodegradable organics, filtrate underwent a more extended biological treatment, both aerobic and anaerobic. This aimed at evaluating if

302 the observed inhibitory impacts shown in Fig. 1 (a-d) were related to the recalcitrant or biodegradable
303 fractions.

304 Comparing organics to full-scale unstable filtrate, all COD fractions decreased after 4-day aerobic
305 pretreatment and 12-day anaerobic treatment (compositions shown in Table 1 I and II). For AerAOB, no
306 significant inhibition was observed with the pretreated filtrate, indicating the original loss of AerAOB
307 activity was most likely related to slowly biodegradable COD (Fig. 1.a;e). For AnAOB, however, there
308 was no clear relation between biodegradable COD and activity loss, as AnAOB were still totally inhibited
309 when exposed to more than 30% filtrate (Fig. 1b;f).

310 To further identify the potential inhibitors on AerAOB and possible remedies to avoid such compounds,
311 additional pretreatments were performed, based on the biological (1+2) or chemical nature (3+4+5) of the
312 activity-limiting compounds: (1) micronutrient addition, (2) six-month filtrate storage (4 °C), (3)
313 coagulation/precipitation through iron or zinc addition, (4) extraction using hexane, (5) sorption of
314 specific organics on biochar and activated carbon. Adding extra micronutrients in the filtrate did not
315 mitigate the activity loss (Table 2), indicating that the filtrate composition did not cause growth limitation
316 for the AerAOB. After six-month storage, the filtrate showed an inhibition of 39.0±0.5%, similar to the
317 fresh filtrate indicating that biodegradable organic fraction underwent few changes during storage. As for
318 the pretreatments chemically removing the particular organic fraction, no significant impact was observed
319 for the precipitation with iron or zinc, extraction with solvent or sorption on biochar (Table 2).
320 Interestingly, sorption on activated carbon showed a clear potential of removing the inhibitory compounds
321 for AerAOB. Furthermore, the impact of activated carbon on alleviating AnAOB inhibition was also
322 demonstrated, decreasing the inhibition significantly from 42±6% to 2±6% (at 20% of volume exposure).

323

324 **3.3 Impact of dewatering efficiency**

To understand the impact of colloidal and particulate COD fractions, and to examine the optimal dewatering conditions, changes in flocculant polymer (FLOPAM) dose were tested (Table 1 III), along with dosage variations in polyDADMAC or $FeCl_3$ as coagulants (Table 1 IV and V).

OPD of the flocculant polymer was around 10 g FLOPAM/kg sludge-TS and no improvement in dewatering was observed with a further increase in polymer dose (Fig. 2a). A coagulant (polyDADMAC or $FeCl_3$) was added to differentially capture particulate and colloidal fractions. Dosing polyDADMAC and $FeCl_3$ in addition to 10 g FLOPAM/kg sludge-TS significantly improved the filtrate quality by capturing more particulate and colloidal COD (Fig. 2 b,c). PolyDADMAC captured the large colloids efficiently, reducing $COD_{coll\text{-}L}$ from around 500 to 155 mg COD/L, but could not efficiently capture the small colloids (Fig. 2b, Table 1 IV). $FeCl_3$ captured both large and small colloids, resulting around 200 mg COD/L of small colloids. From a dose of 2 g polyDADMAC/kg sludge-TS and 70 g $FeCl_3$/kg sludge-TS onwards, no additional improvement was observed (Fig. 2 b,c). The biological impact of the presence/absence of these coagulant dosages was therefore tested in the subsequent microbial activity tests.

For AerAOB, dewatering without coagulants, i.e. using only FLOPAM during dewatering, yielded a filtrate composition with around 1200 mg COD_{part}/L, 500 mg $COD_{coll\text{-}L}$/L and 400 mg $COD_{coll\text{-}S}$/L (Fig. 2a). The lowest AerAOB inhibition (13±8%) was obtained at an optimal FLOPAM dose of 10 g FLOPAM/kg sludge-TS (Fig. 3 a). Underdosing of polymer (7 g FLOPAM/kg sludge-TS) led to an increase in particulate and colloidal COD content in the filtrate and an AerAOB inhibition of 36.7±8.9%. However, overdosing (14 g FLOPAM/kg Sludge-TS) also lowered AerAOB rates by 31.4±7.9%, which might have been caused by the presence of residual polymer potentially creating oxygen uptake limitation due to diffusion resistance (Fig. 3a).

Adding coagulant only improved the AerAOB activity in the case of polyDADMAC. The addition of polyDADMAC efficiently captured the large colloidal fraction, as indicated above, lowering the AerAOB

inhibition to a minimum for filtrate from unstable full-scale THP-AD operation (Fig. 3c, Table 1 IV, V). A similar experiment was performed under stable AD performance as shown in Fig. 3c. As a lower large colloidal fraction was automatically obtained under stable AD (Table 1 IV, V), AerAOB rates were not improved significantly (Fig. 3c). Though $FeCl_3$ captured both large and small colloids, no clear improvement in the AerAOB activity was observed (Fig. 3c), which might relate to the potential impact of excess $FeCl_3$ in the filtrate. Therefore, assuming 10% of the dosed $FeCl_3$ would remain in the filtrate, an additional batch test was performed by adding 333 mg $FeCl_3$/L to filtrate only dewatered by flocculant polymer dose. Higher AerAOB activity loss at $FeCl_3$ dosing was observed; 34±10% compared to 21±4% activity loss when exposed to filtrate only dosed by FLOPAM, confirming the hypothesis of harmful residual $FeCl_3$.

As the previous experiments optimized FLOPAM dose before coagulant dose (polyDADMAC), this was reverted in an additional experiment. Results in Fig. 2b pointed at 2 g polyDADMAC/kg sludge-TS as a minimum to improve the capture efficiency of large colloidal COD. Additional dewatering tests showed that the presence of this coagulant level increased the capture efficiency for particulate and colloidal matter increased, enabling to lower the flocculant dose (Fig. 4 a,b). Indeed, the capture efficiency of large colloids increased to 70-80% at total polymer dose of 6.2 g polymer/kg sludge-TS, i.e. containing 4.2 g FLOPAM/g sludge-TS (Fig. 4b). However, in the absence of polyDADMAC, about 9 g FLOPAM/kg sludge-TS was needed to achieve a similar effect (Fig. 4a).

For AnAOB, in all dewatering tests, no substantial improvements on AnAOB rates were achieved (Fig. 3b;d), indicating that particulate and colloidal COD potentially did not play a major role in AnAOB inhibition.

3.3 Model-based mechanisms of lowered activities

In order to identify the mechanisms lowering AerAOB and AnAOB activities, different model types were fitted to the data obtained from the batch experiments. As only short-term testing was performed in this study, the focus was on identification of direct inhibition impacts (K'_I impacts) and diffusion impacts (K'_S impacts).

Model class 1 was based on direct inhibitors (I), assuming diffusion limitations were independent of the inhibitor: COD fractionating was not considered: $I = COD_{tot}$. The conventional Monod approach was used in model 1a (S.eq. 1), while model 1b incorporated a minimum function yielding full impact of the rate-limiting step (S.eq. 2) (Supplementary material S2 and S3). Model 1a estimated K'_I values of 1519±155 and 269±32 mg COD_{tot}/L for AerAOB and AnAOB, respectively (Table 3, Fig. 5). With Model 1b, slightly lower K'_I values were obtained of 1282±122 and 258±30 mg COD_{tot}/L for AerAOB and AnAOB, respectively. Comparing the goodness of fit of both models, the conventional approach (model 1a) was found superior to the minimum model (model 1b), as the latter yielded higher TSE, MSE and RSE (Table 3).

In model class 2, next to direct inhibitors (I), also diffusional inhibitors (I_d) were taken into account, as compounds influencing the diffusion of substrates and direct inhibitors. To perform a preliminary screening as to which COD fraction corresponds to which inhibitor type, PCA was performed using all batch test data. This revealed that the four COD fractions could be categorized in two or three classes with a differential impact on AerAOB and AnAOB activities: either COD_{diss} + COD_{coll-S} vs. COD_{coll-L} + COD_{part}, or COD_{diss} + COD_{coll-S} vs. COD_{coll-L} vs. COD_{part} (Fig. S.1). Soluble and small colloidal COD were grouped as one fraction and considered to only cause direct inhibition ($I = COD_{diss} + COD_{coll-S}$). For large colloidal and particulate COD, an impact of the diffusion resistance was anticipated, either lumped into one inhibitor in model 2a ($I_d = COD_{part} + COD_{coll-L}$; S.eq. 3) or treated as separate inhibitors in model 2b ($I_{d-1} = COD_{part}$; $I_{d-2} = COD_{coll-L}$; S.eq. 4) (Supplementary material S4 and S5).

When implementing model 2a (S.eq. 3) for AerAOB, the estimated parameters indicated a major sensitivity to compounds causing diffusional resistance, as the K'_I value was considerably lower compared to model 1, and as $K'_{I\text{-}d}$ was considerably lower than K'_I (Table 3). However, despite a slightly lower TSE, model 2a did not render a better fit than model 1, as MSE increased, and the F-test showed no significant improvement ($p > 0.05$). For model 2b, discriminating between the individual contributions by particulate and large colloidal organics, a relatively high $K'_{I\text{-}d}$ value was obtained for COD_{part} and a low value for $COD_{coll\text{-}L}$, indicating that the latter was mainly causing the diffusion resistance. Model 2b provided the best fit for AerAOB inhibition, as obtained TSE and MSE were the lowest, and the F-test showed significant improvement compared to models 1 and 2a ($p \leq 0.05$). Another model fitting was performed by considering small colloidal COD as a diffusional impactor (data not shown). The results predicted a K'_I for $COD_{coll\text{-}S}$ of 2744±405 mg COD/L, a value considerably above the maximum observed concentration of small colloidal COD in THP-AD filtrate. It can, therefore, be concluded that $COD_{coll\text{-}S}$ did not limit substrate diffusion.

For AnAOB, the direct-only inhibition models did not show improvement of including a minimum function (model 1b), as TSE and MSE did not lower compared to model 1a (Table 3). Furthermore, the inclusion of diffusional limitation in model 2 yielded no significant improvement in fit, as shown by the F-tests ($p > 0.05$; Table 3). Models 2a and 2b estimated relatively low and high values for K_{Id} and K_{Ind}, respectively, indicating indeed that diffusion resistance was limited (Table 3).

4. Discussion

4.1 Organics inhibiting AerAOB

THP-AD filtrate caused direct AerAOB inhibition linked to biodegradable dissolved organic compounds, excluding acetate. The model however indicated AerAOB were less sensitive to soluble compounds than

AnAOB, with an estimated K'_I for $COD_{diss+coll-S}$ about 4 times above the one for AerAOB. The AerAOB inhibition could be mitigated by extended biological treatment (aerobic or anaerobic) or activated carbon adsorption. The latter process is widely used to adsorb polar compounds, for instance in soil remediation, removing hydrophobic organic contaminants and polychlorinated biphenyls (Hale et al. 2013, Marchal et al. 2013, Vasilyeva et al. 2006). It is unclear why biochar could not overcome AerAOB inhibition though it has similar properties. In theory, each of the three options could be implemented to lower the biodegradable COD content in THP-AD filtrate, (i) by treating the filtrate aerobically, e.g. in a trickling filter, (ii) by extending the SRT in AD, e.g. with a post-digester, or (iii) by installing an activated carbon process. However, such pretreament approaches require an additional unit process and are not practically feasible or cost-effective. Preferentially the inhibition can be prevented or cured by altering the operation of the existing processes, e.g. by increasing the aerobic SRT or the dilution of the filtrate. Additional clues are expected from a deeper analytical characterization of differences in dissolved organics in THP-AD vs. conventional AD filtrate.

Besides the direct effect, the filtrate's organics also indirectly lowered the AerAOB activity, with particulates and large colloids putatively limiting the diffusion of substrates. A clear relationship between the dewatering performance and AerAOB activities was shown, similar to earlier studies showing the important influence of diffusion on nitrification kinetics in practice, for instance in case of an increased solids load to the system during storm events (Armstrong, 2008; Shaw et al., 2015; Stenstrom and Poduska, 1980). Optimizing flocculant polymer dose to reduce residue solids or polymer in THP-AD filtrate diminished the AerAOB inhibition (Fig. 3.a). This is in line with observations in full-scale operation of sidestream deammonification, where a high TSS inflow led to decreased turnover rates of AerAOB and nitrite oxidizing bacteria (NOB), and restoring of the AerAOB activity was achieved after doubling the aeration time and increasing the DO concentration of up to 1 mg O_2/L (Joss et al. 2011). In contrast to the under-dosed filtrate, the polymer residue in the over-dosed filtrate can cause foaming issues and potentially diffusion limitations, as observed in 30% of the plants (Lackner et al. 2014). In

443 contrast to the under-dosed filtrate, the polymer residue in the over-dosed filtrate can cause foaming
444 issues and potentially diffusion limitations, as observed in 30% of the plants (Lackner et al. 2014). The
445 impact of foaming on reactor performance created substrate intake limitation and the recovery usually
446 takes about1-5 days confirming that the system is not inhibited.

447 The AerAOB inhibition from large colloids could be significantly prevented, although not completely
448 removed, by optimizing the dewatering stage, i.e. adding coagulant to better capture this fraction,
449 especially during unstable digestion (Fig. 3c). Model 2b showed that separating the particle sizes (0.45 to
450 1 µm vs. > 1µm) led to a relatively low K'_I value for large colloidal COD (7.6 ±1.3 mg COD_{coll-L} /L),
451 pinpointing this fraction as a key inhibitor class to AerAOB. Compared to the typical content of large
452 colloids in THP-AD filtrate (211±151 mg COD_{coll-L}/L), the low K'_I indicated that the large colloidal
453 fraction was the rate-limiting factor. Under high levels of colloidal matter, oxygen transfer efficiency
454 decreased, resulting in limited DO availability and consequently a poor nitrification performance
455 (Germain et al. 2007, Wu et al. 2013). Li et al. (2018) observed the decrease of oxygen availability
456 lowered substrate conversion in biofilms due to the high loadings of particulate organics in wastewater,
457 which resulted in 20-70% of dissolved oxygen flux reduction from the biofilm surface into biofilm matrix.
458 Coagulants neutralize the negative electric charge on particles and destabilize the forces keeping colloids
459 apart (Poon and Chu 1999). The large colloidal fractions, in the case of THP-AD filtrate, had more impact
460 on AerAOB flocs possible due to the relative small AerAOB floc size compared to the AnAOB granules
461 (Han et al. 2016, Vlaeminck et al. 2010)., ~~and~~ The diffusion impact on the AerAOB-containing flocs was
462 relatively dominant, creating diffusion limitation of substrates, e.g. oxygen or ammonium, rather than
463 directly impacting the cell's metabolism or growth rate negatively. The curative strategy of increasing the
464 DO level helps to overcome diffusion limitation and improve ammonium removal rates as confirmed by
465 Zhang et al. (2016). Additionally, unlike the inhibition related to the soluble factions, the lowered
466 AerAOB rates caused by diffusion limitation are usually transient, reversible and easy to notice.

Adequate trace nutrient concentrations, including metal ions and vitamins, are necessary to have a diverse microbial community thrive in an activated sludge plant, especially when treating certain types of industrial wastewater (Burgess et al. 1999, Jefferson et al. 2001). Klein et al. (2013) and Nifong et al. (2013) observed a full-scale sidestream deammonification system instability due to the micronutrient limitations. The activity test in this study showed that the biomass inhibition was not related to acute micronutrient deficiency (Table 2). Long-term operation is, however, necessary to validate if adding extra bioavailable micronutrients might be helpful to compensate for the decreased growth rates and/or increased decay rates.

4.2. Organics inhibiting AnAOB

For AnAOB, the kinetic tests indicated that soluble organics in THP-AD filtrate were the primary source of inhibition, potentially related to the nonbiodegradable fraction. Concentrations of dissolved organics were tightly related to THP and AD operation stability. However, due to the multitude and complexity of the organics, it is an analytical challenge to identify the specific inhibitors. Dwyer et al. (2008) reported an increased presence of recalcitrant organic compounds in THP-AD filtrate was related to the pretreatment at an excessively high temperature (higher than 170 – 190°C) which led to significant changes in a generation of recalcitrant N and COD. Meanwhile, these soluble inhibitory organics were not easily removed via aerobic and anaerobic treatment as the remaining AnAOB activity was lower than 80% (Fig. 1f). Gupta et al. (2015) showed that organic matter in the THP-AD filtrate could not be efficiently removed by aerobic biological treatment. The biodegradable organics related to the digester instability increased inhibition and can be caused by variable (e.g. shock) loading, resulting in partial sludge degradation and associated accumulation of surface active substances and subsequent foaming issues (Ganidi et al. 2009). The total nitrogen removal rate in a lab-scale sidestream deammonification system decreased with 90% resulting in substantial nitrite accumulation (> 20 mg NO_2^--N/L) when fed with

filtrate containing increased soluble organics (5934±680 mg COD/L) caused by digester overloading (Zhang et al. 2016). An increase in VFA concentration usually occurs as an indicator and consequence of unstable AD (Chen et al. 2008, Iv 2003), as also seen in this study with an increase of soluble COD from 2762 mg COD/L to 6600 mg COD/L in the filtrate, with around 35% of the increase due to acetate. However, actual VFA concentrations in unstable filtrate were a lot lower than the inhibitory levels for AnAOB observed in previous studies (Dapena-Mora et al. 2004, Molinuevo et al. 2009). In comparison to our acetate value of 1.3 g COD/L in unstable THP-AD filtrate, Kindaichi et al. (2016) observed that concentrations up to 3.2 g COD/L of acetate had no effects on AnAOB. The acetate spike test at 1.3 g COD/L also confirmed no impact on the AnAOB activity (Fig. 1d).

Model runs confirmed the sensitivity of AnAOB towards soluble COD. The estimated K'_I of 250 mg COD/L is 4 times lower than the toxicity level at 800 mg COD/L observed in the long-term SBR operation (Zhang et al. 2016). This higher level can relate to an underloaded AnAOB inventory resulting from efficient AnAOB retention in the SBR. However, once inhibition has been observed in sidestream deammonification, it usually takes the biomass a month to recover. Therefore, longer SRT and good AnAOB retention are necessary to compensate for the decreased growth rates. Furthermore, even with actions taken in THP and AD, improvements in filtrate composition lag because of the long SRT in AD. Thus, monitoring the digesters' performance is important, and upon instability, manifested by less methane, foaming, more VFA and ammonia, etc., it is necessary to dilute the filtrate more. The full-scale deammonification system at DC Water is designed to treat THP-AD at a 1:1 dilution ratio with water (Zhang et al. 2016). The potential drawback of a higher dilution is the temperature loss, especially in winter time.

5. Conclusion

514 This paper investigated four organic fractions in the filtrate from anaerobic digestion preceded by thermal
515 hydrolysis, to identify specific inhibition compounds and mechanisms for AerAOB and AnAOB.
516 Furthermore, the findings were confronted with a global mechanistic inhibition model. AerAOB were
517 inhibited directly, from dissolved organics, and indirectly, with particulate and colloidal fractions causing
518 diffusion limitation. The latter can be resolved through optimization of the dewatering process in terms of
519 flocculant and coagulant polymer dosing, to obtain a better capture of the colloidal fraction to the sludge
520 cake. An inhibition model including diffusion resistance based on the porter-equation showed the best fit
521 with the experimental data, and highlighted that AerAOB were highly sensitive to large colloids. For
522 AnAOB, it was found activity was mainly impacted by dissolved organics in the filtrate, tightly linked to
523 the THP and digester performance, not by changes in the dewatering process.

524

525 **Acknowledgements**

526 This work was supported by District of Columbia Water and Sewer Authority, Washington, DC. The
527 authors gratefully thank Norman Dockett for technical support, and everyone in the DC Water research
528 lab for all assistance offered.

529

530 **References**

531 Al-Omari, A., Wett, B., Nopens, I., De Clippeleir, H., Han, M., Regmi, P., Bott, C. and Murthy, S. (2015)
532 Model-based evaluation of mechanisms and benefits of mainstream shortcut nitrogen removal
533 processes. Water Sci Technol 71(6), 840-847.
534 Bader, F.G. (1978) Analysis of double-substrate limited growth. Biotechnol Bioeng 20(2), 183-202.
535 Barber, W.P.F. (2016) Thermal hydrolysis for sewage treatment: A critical review. Water Res 104, 53-71.
536 Beg, S.A. and Hassan, M.M. (1987) Effects of inhibitors on nitrification in a packed-bed biological flow
537 reactor. Water Research 21(2), 191-198.
538 Bougrier, C., Delgenès, J.P. and Carrère, H. (2008) Effects of thermal treatments on five different waste
539 activated sludge samples solubilisation, physical properties and anaerobic digestion. Chemical
540 Engineering Journal 139(2), 236-244.
541 Burgess, J.E., Quarmby, J. and Stephenson, T. (1999) Micronutrient supplements for optimisation of the
542 treatment of industrial wastewater using activated sludge. Water Research 33(18), 3707-3714.
543 Chan, A.A. (2015) Experience with Anammox Sludge Liquor Treatment and Up-Coming Challenges with
544 Thermal Hydrolysis Effluents at the Sundet Wwtp, Vaxjo/ Sweden, pp. 1-11, Washington DC.

545 Chen, Y., Cheng, J.J. and Creamer, K.S. (2008) Inhibition of anaerobic digestion process: a review.
546 Bioresour Technol 99(10), 4044-4064.
547 Dapena-Mora, A., Campos, J.L., Mosquera-Corral, A. and Mendez, R. (2006) Anammox process for
548 nitrogen removal from anaerobically digested fish canning effluents. Water Sci Technol 53(12), 265-274.
549 Dapena-Mora, A., Van Hulle, S.W.H., Luis Campos, J., Méndez, R., Vanrolleghem, P.A. and Jetten, M.
550 (2004) Enrichment of Anammox biomass from municipal activated sludge: experimental and modelling
551 results. Journal of Chemical Technology & Biotechnology 79(12), 1421-1428.
552 Dwyer, J., Starrenburg, D., Tait, S., Barr, K., Batstone, D.J. and Lant, P. (2008) Decreasing activated sludge
553 thermal hydrolysis temperature reduces product colour, without decreasing degradability. Water Res
554 42(18), 4699-4709.
555 Feng, G., Tan, W., Zhong, N. and Liu, L. (2014) Effects of thermal treatment on physical and expression
556 dewatering characteristics of municipal sludge. Chemical Engineering Journal 247, 223-230.
557 Figdore, B., Wett, B., Hell, M., Murthy, S., Bowden, G. and Stinson, B. (2011) Treatment of dewatering
558 sidestream from a thermal hydrolysis-mesophilic anaerobic digestion process with a single-sludge
559 deammonification process, pp. 249-264.
560 Florent Baty, Marie-Laure, Delignette-Muller, Sandrine Charles, Jean-Pierre Flandrois and Ritz, C. (2015)
561 Package 'nlstools', pp. R package version 1.0-2.
562 Francois Husson, Julie Josse, Sebastien Le and Mazet, J. (2018) Package 'FactoMineR', p. R package
563 version 1.41.
564 Ganidi, N., Tyrrel, S. and Cartmell, E. (2009) Anaerobic digestion foaming causes--a review. Bioresour
565 Technol 100(23), 5546-5554.
566 Ganigué, R., López, H., Ruscalleda, M., Balaguer, M.D. and Colprim, J. (2008) Operational strategy for a
567 partial nitritation–sequencing batch reactor treating urban landfill leachate to achieve a stable influent
568 for an anammox reactor. Journal of Chemical Technology & Biotechnology 83(3), 365-371.
569 Germain, E., Nelles, F., Drews, A., Pearce, P., Kraume, M., Reid, E., Judd, S.J. and Stephenson, T. (2007)
570 Biomass effects on oxygen transfer in membrane bioreactors. Water Res 41(5), 1038-1044.
571 Gujer, W. (2010) Nitrification and me - a subjective review. Water Res 44(1), 1-19.
572 Gupta, A., Novak, J.T. and Zhao, R. (2015) Characterization of organic matter in the thermal hydrolysis
573 pretreated anaerobic digestion return liquor. Journal of Environmental Chemical Engineering 3(4), 2631-
574 2636.
575 Hale, S.E., Jensen, J., Jakob, L., Oleszczuk, P., Hartnik, T., Henriksen, T., Okkenhaug, G., Martinsen, V. and
576 Cornelissen, G. (2013) Short-term effect of the soil amendments activated carbon, biochar, and ferric
577 oxyhydroxide on bacteria and invertebrates. Environ Sci Technol 47(15), 8674-8683.
578 Han, K. and Levenspiel, O. (1988) Extended monod kinetics for substrate, product, and cell inhibition.
579 Biotechnol Bioeng 32(4), 430-447.
580 Han, M., Vlaeminck, S.E., Al-Omari, A., Wett, B., Bott, C., Murthy, S. and De Clippeleir, H. (2016)
581 Uncoupling the solids retention times of flocs and granules in mainstream deammonification: A screen
582 as effective out-selection tool for nitrite oxidizing bacteria. Bioresour Technol 221, 195-204.
583 Haug, R.T. (1978) Sludge Processing to Optimize Digestibility and Energy Production. Water Pollution
584 Control Federation 49(7), 1713-1721.
585 Iv, P. (2003) Process Control and Troubleshooting.
586 Jefferson, B., Burgess, J.E., Pichon, A., Harkness, J. and Judd, S.J. (2001) Nutrient addition to enhance
587 biological treatment of greywater. Water Res 35(11), 2702-2710.
588 Jolis, D. (2008) High-solids anaerobic digestion of municipal sludge pretreated by thermal hydrolysis.
589 Water Environ Res 80(7), 654-662.
590 Joss, A., Derlon, N., Cyprien, C., Burger, S., Szivak, I., Traber, J., Siegrist, H. and Morgenroth, E. (2011)
591 Combined nitritation-anammox: advances in understanding process stability. Environ Sci Technol 45(22),
592 9735-9742.

Kindaichi, T., Awata, T., Mugimoto, Y., Rathnayake, R., Kasahara, S. and Satoh, H. (2016) Effects of organic matter in livestock manure digester liquid on microbial community structure and in situ activity of anammox granules. Chemosphere 159, 300-307.
Klein, A., Williams, L., Summers, A., Johnson, C. and Melcer, H. (2013) Application of Lessons Learned During a Pilot Investigation to the Full Scale Design of a DEMON ⓒ System to Remove Nitrogen from Dewatering Centrate, pp. 350-364b(315), Water Environment Federation.
Lackner, S., Gilbert, E.M., Vlaeminck, S.E., Joss, A., Horn, H. and van Loosdrecht, M.C. (2014) Full-scale partial nitritation/anammox experiences--an application survey. Water Res 55(0), 292-303.
Li, C., Brunner, F., Wagner, M., Lackner, S. and Horn, H. (2018) Quantification of particulate matter attached to the bulk-biofilm interface and its influence on local mass transfer. Separation and Purification Technology 197, 86-94.
Lotti, T., Cordola, M., Kleerebezem, R., Caffaz, S., Lubello, C. and van Loosdrecht, M.C. (2012) Inhibition effect of swine wastewater heavy metals and antibiotics on anammox activity. Water Sci Technol 66(7), 1519-1526.
Marchal, G., Smith, K.E., Rein, A., Winding, A., Wollensen de Jonge, L., Trapp, S. and Karlson, U.G. (2013) Impact of activated carbon, biochar and compost on the desorption and mineralization of phenanthrene in soil. Environ Pollut 181, 200-210.
Molinuevo, B., Garcia, M.C., Karakashev, D. and Angelidaki, I. (2009) Anammox for ammonia removal from pig manure effluents: effect of organic matter content on process performance. Bioresour Technol 100(7), 2171-2175.
Nifong, A., Nelson, A., Johnson, C. and Bott, C.B. (2013) Performance of a Full-Scale Sidestream DEMON Deammonification Installation, Vancouver.
Niu, M., Zhang, W., Wang, D., Chen, Y. and Chen, R. (2013) Correlation of physicochemical properties and sludge dewaterability under chemical conditioning using inorganic coagulants. Bioresour Technol 144, 337-343.
Pickworth, B., Adams, J., Panter, K. and Solheim, O. (2006) Maximising biogas in anaerobic digestion by using engine waste heat for thermal hydrolysis pre-treatment of sludge. Water Science and Technology 54(5), 101-108.
Poon, C.S. and Chu, C.W. (1999) The use of ferric chloride and anionic polymer in the chemically assisted primary sedimentation process. Chemosphere 39(10), 1573-1582.
Shaw, A.R., Takacs, I., Pagilla, K., Riffat, R., De Clippeleir, H., Wilson, C. and Murthy, S. (2015) Toward Universal Half-Saturation Coefficients: Describing Extant KS as a Function of Diffusion. Water Environment Federation 87(5), 387-387.
Sinha, B. and Annachhatre, A.P. (2006) Partial nitrification—operational parameters and microorganisms involved. Reviews in Environmental Science and Bio/Technology 6(4), 285-313.
Stewart, H.A., Al-Omari, A., Bott, C., De Clippeleir, H., Su, C., Takacs, I., Wett, B., Massoudieh, A. and Murthy, S. (2017) Dual substrate limitation modeling and implications for mainstream deammonification. Water Res 116, 95-105.
Timur V. Elzhov, Katharine M. Mullen, Andrej-Nikolai Spiess and Bolker, B. (2016) Package 'minpack.lm', pp. R package version 1.2-1.
Vasilyeva, G.K., Strijakova, E.R. and Shea, P.J. (2006) Soil and Water Pollution Monitoring, Protection and Remediation. Twardowska, I., Allen, H.E., Häggblom, M.M. and Stefaniak, S. (eds), pp. 309-322, Springer Netherlands, Dordrecht.
Vlaeminck, S.E., Terada, A., Smets, B.F., De Clippeleir, H., Schaubroeck, T., Bolca, S., Demeestere, L., Mast, J., Boon, N., Carballa, M. and Verstraete, W. (2010) Aggregate size and architecture determine microbial activity balance for one-stage partial nitritation and anammox. Appl Environ Microbiol 76(3), 900-909.

640 Wu, Y.J., Whang, L.M., Chang, M.Y., Fukushima, T., Lee, Y.C., Cheng, S.S., Hsu, S.F., Chang, C.H., Shen, W.,
641 Yang, C.Y., Fu, R. and Tsai, T.Y. (2013) Impact of food to microorganism (F/M) ratio and colloidal
642 chemical oxygen demand on nitrification performance of a full-scale membrane bioreactor treating thin
643 film transistor liquid crystal display wastewater. Bioresour Technol 141, 35-40.
644 Zhang, Q., De Clippeleir, H., Su, C., Al-Omari, A., Wett, B., Vlaeminck, S.E. and Murthy, S. (2016)
645 Deammonification for digester supernatant pretreated with thermal hydrolysis: overcoming inhibition
646 through process optimization. Appl Microbiol Biotechnol 100(12), 5595-5606.

647

Legends

Figure 1. Impact of different dilutions of raw and treated THP-AD filtrate on AerAOB (a, c, e) and AnAOB activities (b, d, f), originating from different digesters and performance status (a, b, c, d; Table 1 I), linked to the impact of acetate dosing (c, d) and biological pre-treatment: 1-day aerobic treatment (c, d); 7-day aerobic treatment and 12-day anaerobic treatment (e, f).

Figure 2. Impact of chemical dosing in THP-AD sludge dewatering (filtration) on COD fractionation and TSS levels: dose of flocculant FLOPAM (a-1, a-2) and variation in coagulant doses at optimal flocculant dose (10 g FLOPAM/kg sludge-TS), using polyDADMAC (b-1, b-2) or $FeCl_3$ (c-1, c-2). The selected filtrate used for the subsequent activity tests (Figure 3) was marked with *.

Figure 3. Impacts on AerAOB (a, c) and AnAOB (b, d) activities of chemicals added in full-scaleTHP-AD sludge dewatering (filtration): dose of flocculant FLOPAM (a, b; Table 1 III; 30% filtrate based on volume) and variation in coagulant at optimal flocculant dose (10 Gflopam/kg Sludge-TS), using polyDADMAC or $FeCl_3$, linked to digester stability (c, d; Table 1 IV,V; 20% filtrate based on volume). Significantly improved activity was marked with * ($p \leq 0.05$).

Figure 4. Impact of the cationic polymer dose on the capture efficiencies of suspended solids (TSS), particulate organics (COD_{part}) and large colloidal organics (COD_{coll-L}) to the cake fraction during digestate dewatering: flocculant polymer (FLOPAM) dosing in absence of polyDADMAC (a) and presence of 2 g polyDADMAC/kg sludge-TS.

Figure 5. Model fitting comparisons of direct inhibition models (Model 1 a, b) with direct and diffusional inhibition models (Model 2 a, b) for AerAOB (a) and AnAOB (b) (model parameters displayed in Table 3.

670

671 Table 1. Composition of filtrate from anaerobic digestion (AD) of sewage sludge pre-treated with a thermal hydrolysis process (THP) as a function of
672 its origin and post-treatment (aerobic/anaerobic, flocculation, coagulation) based on 97 batch tests. a. particulate COD; b. large colloidal COD; c.
673 small colloidal COD; d. soluble COD, e. volatile fatty acid, f. measurement including COD_{coll-s} + COD_{diss}, g. not available, h. not detectable

	Test description		*Composition (No dilution)*							Refer to Figure
#			Polymer dose	NH_4^+	COD_{part} [a]	COD_{coll-L} [b]	COD_{coll-S} [c]	COD_{diss} [d]	VFA [e]	
			g/kg sludge-TS	mg N/L	mg/L	mg/L	mg/L	mg/L	mg COD/L	
I	Different THP-AD sludge at different phases	Lab-scale AD	14	1910	158	399		2830[f]	70	Fig. 1
		Full-scale AD (stable)	10	1882	381	243	219	2762	50	
		Full-scale AD (unstable, start-up phase)	10	1925	550	450	825	6600	1502	
II	Biodegradable COD	1-day aerobic treatment (25°C)	14	N.A.[g]	56	366		3896[f]		
		7-days aerobic treatment (25°C)	10	593	535	120	415	3175	N.D.[h]	Fig. 1
		12-day anaerobic treatment (38°C)	17	2235	325	230	200	2680	N.D.	
III	Optimizing flocculant polymer dose	Under-dose (FLOPAM)	7	1883	587	937		3454[f]	68	Fig. 3
		Optimum dose (FLOPAM)	10	1885	218	76		3670[f]	61	
		Over-dose (FLOPAM)	14	1800	148	32		3758[f]	77	
IV	Coagulant addition to unstable full-scale digester sludge	FLOPAM	0+10	2217	1275	515	415	3770	N.A.	Fig. 3
		PolyDADMAC +FLOPAM	2+10	2205	895	155	425	3775	N.A.	
		$FeCl_3$+FLOPAM	0.07+10	2170	685	220	170	3395	N.A.	
V	Coagulant addition to stable full-scale digester sludge	FLOPAM	0+10	1793	478	222	394	2694	55	Fig. 3
		PolyDADMAC +FLOPAM	2+10	1688	286	114	502	2684	45	
		$FeCl_3$+FLOPAM	0.07+10	1752	240	68	134	2640	44	

674

675 Table 2. Overview of the AerAOB inhibition caused by raw and treated THP-AD filtrate. A statistically

676 improved activity compared to the reference was marked with * ($p \leq 0.05$).

Test category	Filtrate description or treatment	AerAOB activity (%)	
		25% filtrate	30% filtrate
Reference	Raw filtrate (stable full-scale AD)		***61*±3***
Growth limitation	Micronutrient addition to raw filtrate		60±1
Presence of VFA and other biodegradable compounds	Raw filtrate (unstable AD, 4000 mg VFA-COD/L)	50±13	
	Raw filtrate (stable AD); acetate spike (1250 mg COD/L)	0±11	
Removal of biodegradable compounds	1-days aerobic treatment (25°C)	37±3	
	7-day aerobic treatment (25°C)	**100±7***	
	12-day anaerobic treatment (38°C)		**100±9***
	6-month storage of raw filtrate (4°C)		39±1
Coagulation of organics /precipitation of anions	Fe(III) dosage (1 g/L); centrifuged		38±11
	Zn(II) dosage (1g/L); centrifuged		97±1
Removal of (apolar) organics	Extraction with hexane		42±1
	Sorption with biochar (40 g/L); centrifuged		39±1
	Sorption with granular activated carbon; centrifuged		**94±12***

677

Table 3. Overview of two approaches for AerAOB and AnAOB parameter estimation. For AerAOB, the apparent oxygen half-saturation without addition change due to I_d was set at 0.25 mg O_2/L, and similarly for AnAOB the apparent nitrite half-saturation was set at 0.5 mg NO_2^--N/L. The two direct inhibition models (Models 1a and b) do not include diffusion limitation. Model 2 incorporates diffusion limitation as additional inhibition mechanism. Firstly particulate COD and large colloidal COD were grouped together as one inhibitory compound (I_d) affecting the diffusion resistance, while soluble COD was considered as inhibitory compound without diffusion impacts (I_{nd}) (Model 2a). A second parameter estimation was performed by considering particulate and large colloidal COD as two individual diffusion-affecting compounds (I_{d1} and I_{d2}, respectively) (Model 2b). Lower values for total and mean summed errors (TSE and MSE) indicate a better goodness of fit, and significant parameter estimation improvements are obtained with F-test p values ≤ 0.05 (*).

	Estimated Parameter	Value	Data range	TSE	MSE	F-test p value
AerAOB						
1 Direct inhibition model: $I = COD_{tot}$						
1a Conventional	R_{max} (mg N/g VSS/h)	25.7±0.6	4.3-30.6	900	9.4	
	K'_I (mg COD_{tot}/L)	1519±155	0-3876			
1b Minimum	R_{max} (mg N/g VSS/h)	25.3±0.7	4.3-30.6	918	9.6	
	K'_I (mg COD_{tot}/L)	1282±122	0-3876			
2 Direct and diffusional inhibition model: $I = COD_{diss} + COD_{coll-S}$						
2a Lumped diffusional inhibitor: $I_d = COD_{part} + COD_{coll-L}$	R_{max} (mg N/g VSS/h)	26.2±0.7	4.3-30.6	889	9.4	0.367***** (2a vs. 1a)
	K'_I (mg $COD_{diss+coll-S}$/L)	826±136	0-3416			
	K'_{I_d} (mg $COD_{part+coll-L}$/L)	25.0±4.1	0-460			
2b Separate diffusional inhibitors: $I_{d1} = COD_{part}$; $I_{d2} = COD_{coll-L}$	R_{max} (mg N/g VSS/h)	26.1±1.0	4.3-30.6	813	8.6	0.035 (2b vs. 1a) 0.001 (2b vs. 2a)
	K'_I (mg $COD_{diss+coll-S}$/L)	890±199	0-3416			
	K'_{I_d1} (mg COD_{part}/L)	5 E+8±4 E+21	0-253			
	K'_{I_d2} (mg COD_{coll-L}/L)	7.6±1.3	0-207			
AnAOB						
1 Direct inhibition model: $I = COD_{tot}$						
1a Coventional	R_{max} (mg N/g VSS/h)	10.0±0.5	0-11.6	174	2.1	
	K'_I (mg COD_{tot}/L)	270±32	0-3876			
1b Minimum	R_{max} (mg N/g VSS/h)	10.0±0.5	0-11.6	176	2.1	
	K'_I (mg COD_{tot}/L)	258±30	0-3876			
2 **Direct and diffusional inhibition model:** $I = COD_{diss} + COD_{coll-S}$						
2a Lumped diffusional inhibitor: $I_d = COD_{part} + COD_{coll-L}$	R_{max} (mg N/g VSS/h)	10.1±0.5	0-11.6	166	2.0	0.051 (eq.6 compared to eq.4)
	K'_I (mg $COD_{diss+coll-S}$/L)	238±27	0-3416			
	K'_{I_d} (mg $COD_{part+coll-L}$/L)	1. E09±2. E 22	0-460			
2b Separate diffusional inhibitors: $I_{d1} = COD_{part}$; $I_{d2} = COD_{coll-L}$	R_{max} (mg N/g VSS/h)	10.1±0.9	0-11.6	166	2.0	0.124 (eq.7 compared to eq.4) 1.000 (eq.7 compared to eq.6)
	K'_I (mg $COD_{diss+coll-S}$/L)	238±39	0-3416			
	K'_{I_d1} (mg COD_{part}/L)	5. E±9±4. E+22	0-253			
	K'_{I_d2} (mg COD_{coll-L}/L)	3. E+10±2. E±21	0-207			

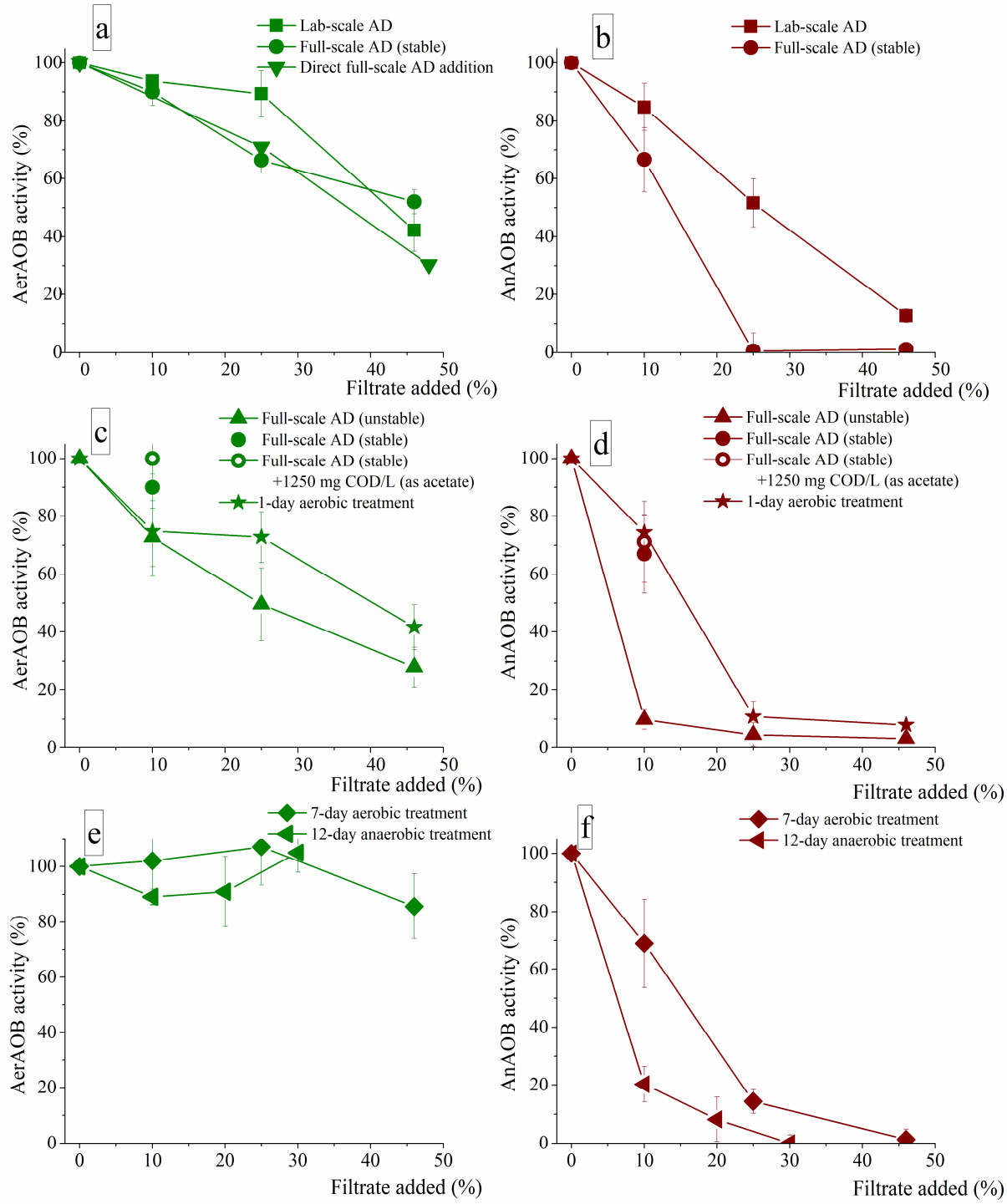
a
Lab-scale AD
Full-scale AD (stable)
Direct full-scale AD addition
AerAOB activity (%)
Filtrate added (%)
b
Lab-scale AD
Full-scale AD (stable)
AnAOB activity (%)
Filtrate added (%)
c
Full-scale AD (unstable)
Full-scale AD (stable)
Full-scale AD (stable)
+1250 mg COD/L (as acetate)
1-day aerobic treatment
AerAOB activity (%)
Filtrate added (%)
d
Full-scale AD (unstable)
Full-scale AD (stable)
Full-scale AD (stable)
+1250 mg COD/L (as acetate)
1-day aerobic treatment
AnAOB activity (%)
Filtrate added (%)
e
7-day aerobic treatment
12-day anaerobic treatment
AerAOB activity (%)
Filtrate added (%)
f
7-day aerobic treatment
12-day anaerobic treatment
AnAOB activity (%)
Filtrate added (%)

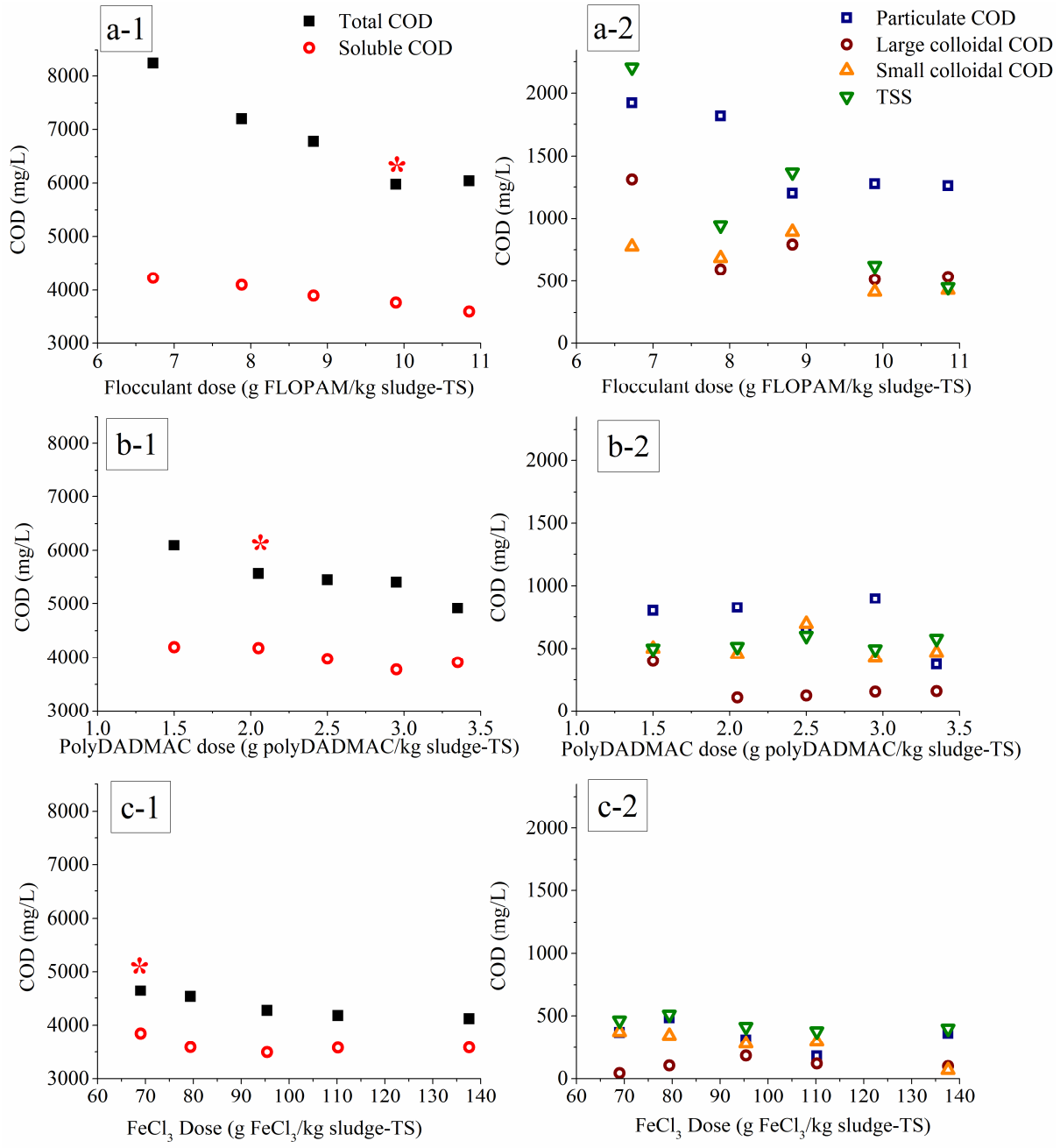
a-1
Total COD
Soluble COD
COD (mg/L)
Flocculant dose (g FLOPAM/kg sludge-TS)
a-2
Particulate COD
Large colloidal COD
Small colloidal COD
TSS
COD (mg/L)
Flocculant dose (g FLOPAM/kg sludge-TS)
b-1
COD (mg/L)
PolyDADMAC dose (g polyDADMAC/kg sludge-TS)
b-2
COD (mg/L)
PolyDADMAC dose (g polyDADMAC/kg sludge-TS)
c-1
COD (mg/L)
FeCl3 Dose (g FeCl3/kg sludge-TS)
c-2
COD (mg/L)
FeCl3 Dose (g FeCl3/kg sludge-TS)

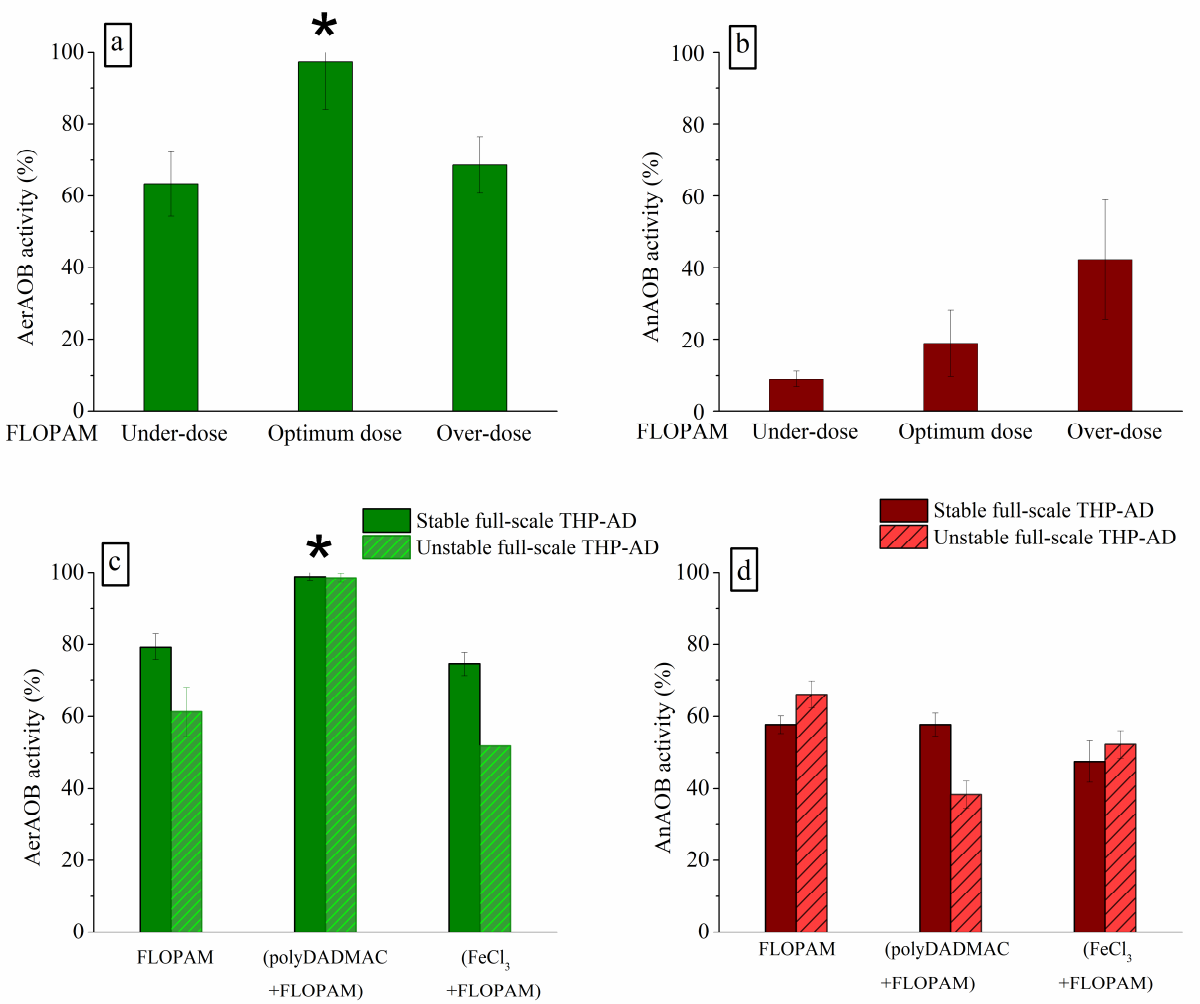
a
*
AerAOB activity (%)
100
80
60
40
20
0
FLOPAM
Under-dose
Optimum dose
Over-dose
b
AnAOB activity (%)
100
80
60
40
20
0
FLOPAM
Under-dose
Optimum dose
Over-dose
c
*
Stable full-scale THP-AD
Unstable full-scale THP-AD
AerAOB activity (%)
100
80
60
40
20
0
FLOPAM
(polyDADMAC +FLOPAM)
($FeCl_3$ +FLOPAM)
d
Stable full-scale THP-AD
Unstable full-scale THP-AD
AnAOB activity (%)
100
80
60
40
20
0
FLOPAM
(polyDADMAC +FLOPAM)
($FeCl_3$ +FLOPAM)

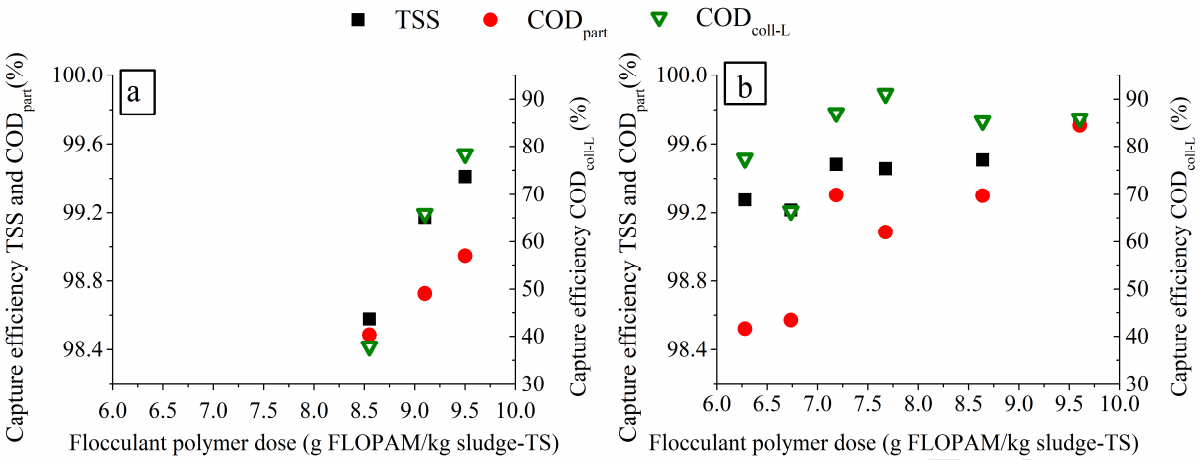

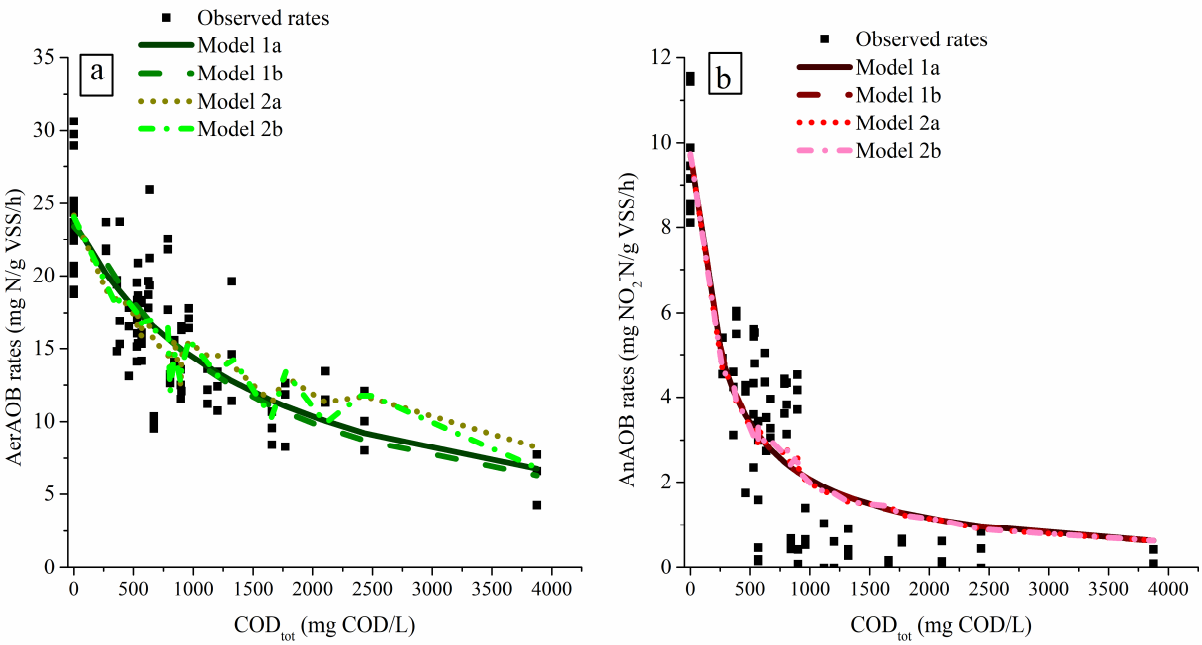

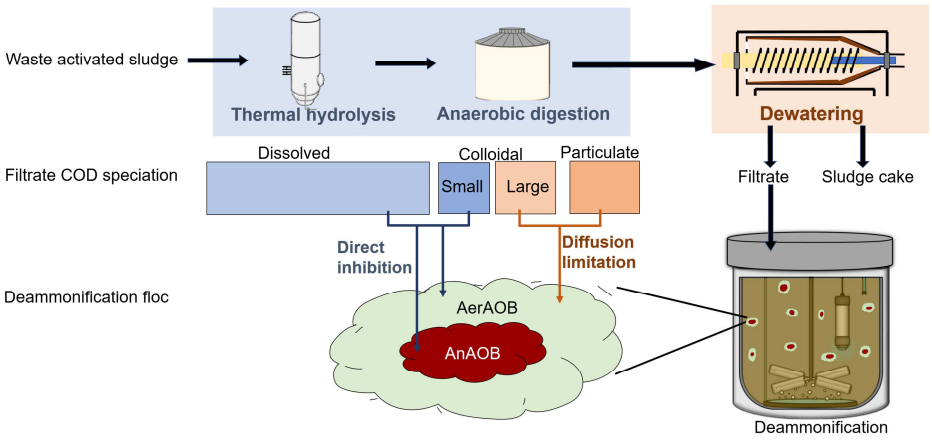

- Four organic fractions quantified in digester filtrate after thermal hydrolysis
- Organics inhibit aerobic and anoxic ammonium-oxidizing bacteria (AerAOB and AnAOB)
- Dissolved organics and small colloids directly inhibit AerAOB and AnAOB
- Large colloids create diffusion resistance indirectly limiting AerAOB activity
- Digester stability and chemically optimized dewatering facilitate deammonification